Progress In Electromagnetics Research C, Vol. 137, 53–64, 2023

Radiation Performance Improvement of a Staircase Shaped Dual Band Printed Antenna with a Frequency Selective Surface (FSS) for Wireless Communication Applications

Nagandla Prasad[1], Pokkunuri Pardhasaradhi[1], Boddapati T. P. Madhav[1, *], Tanvir Islam[2], Sudipta Das[3], and Mohammed El Ghzaoui[4]

Abstract—A staircase-shaped printed monopole antenna (SPMA) with a partial ground structure for wireless applications is proposed. The performance parameters of the designed antenna have been evaluated by integrating a novel structure of frequency selective surface (FSS) with the antenna. A Polyimide dielectric material has been utilized for designing both the antenna and the FSS reflector. The proposed SPMA integrated with designed FSS reflector operates at dual bands from 2.18 to 2.83 GHz and 4.42 to 5.58 GHz with fractional impedance bandwidth of 25.94% and 23.2%, respectively. A single-layered FSS reflector with a 5×5 array size is employed to obtain optimum performance. The suggested combined structure of the FSS reflector integrated staircase antenna achieves an attractive peak gain of 7.87 dBi and radiation efficiency of 98.8%. The design methodology for the antenna and unit cell design of the required FSS, analysis of field and current distributions, fabricated prototyped models of antenna and FSS along with measured results are included and discussed in this article. The proposed antenna is suitable for modern wireless communication (WLAN/Wi-Fi etc.) applications at 2.4/5.2 GHz.

1. INTRODUCTION

The use of microstrip patch antennas for Wi-Fi or any other wireless applications has significantly impacted wireless communications over the last few decades. Traditional patch antennas have several limitations, in terms of limited gain, bandwidth, and radiation efficiency. A few techniques exist for improving the antenna performance, such as adding multiple substrate materials with different dielectric constant values [1], using zigzag feeding [2], using the substrate as a dielectric material with air gap integration [3], changing the design of the patch radiator [4], employing coplanar waveguide (CPW) feed [5], adding more conductive layers on the patch [6], and utilizing the frequency selective surfaces [7]. Frequency selective surface (FSS) is an arrangement of 2D periodic array formation that contains a metal design on a dielectric substrate material. Previous research studies have shown that FSS is beneficial in a variety of ways. For example, it can be used for performance enhancement of the antenna [8], and it can also serve as a sensor [9]. It can be used in medical applications [10], polarization conversion applications [11], and a variety of other applications. The uses of frequency-selective surfaces have been discussed in numerous articles to enhance the performance of the antennas. An FSS is used as a superstrate, and an artificial magnetic conductor (AMC) is used as a plane of reflector. The unit cell size is taken as 4.8 mm which results in a maximum gain of 16 dBi [12]. An FSS is utilized in [13], which contains concentric square loops as a conducting patch for improving its performance; in this

Received 24 July 2023, Accepted 17 August 2023, Scheduled 29 August 2023

* Corresponding author: Boddapati Taraka Phani Madhav (btpmadhav@kluniversity.in).

[1] Antennas and Liquid Crystals Research Center, Department of Electronics and Communication Engineering, Koneru Lakshmaiah Education Foundation, Vaddeswaram, Guntur, Andra Pradesh, India. [2] Department of Electrical and Computer Engineering, University of Houston, Houston, TX 77204, USA. [3] Department of Electronics and Communication Engineering, IMPS College of Engineering and Technology, Malda, W.B, India. [4] Faculty of Sciences, Sidi Mohamed Ben Abdellah University, Fes, Morocco.

case, the antenna size is taken to be $40 \times 40\,\text{mm}^2$, and it will resonate at two different frequencies (2.4, and 5.8 GHz) and achieve a 7.46 dBi gain. A spanner-shaped unit cell is employed to increase the gain of a slot antenna. In this case, the antenna size is taken as $44 \times 35\,\text{mm}^2$, and the FSS as a superstrate is employed which provides a gain of 13.92 dBi, operating for WLAN applications [14]. A triple-layer FSS is employed as a superstrate for the proposed dielectric resonator antenna (DRA) [15], with a size of f $45 \times 42\,\text{mm}^2$, for improving gain and radiation efficiencies. A varactor-loaded square patch antenna with truncated corners is proposed for vehicular communication applications. It has a size of $42.5 \times 28.5\,\text{mm}^2$ and operates at dual resonant frequencies. A cross shape FSS is employed to obtain a peak gain of 13.1 dBi [16].

This article presents a staircase-shaped printed monopole antenna (SPMA), and the performance of this proposed antenna is enhanced by integrating a novel FSS reflector with it. The proposed FSS unit cell structure functions as a reflector and consists of a Jerusalem cross as radiating patches. The proposed SPMA integrated with designed FSS reflector operates at dual bands from 2.18 to 2.83 GHz and 4.42 to 5.58 GHz frequency with fractional impedance bandwidth of 25.94% and 23.2%, respectively. A single-layer FSS reflector with a 5×5 array size is employed to obtain optimum performance. The suggested combined structure of the FSS reflector integrated with the staircase-shaped slot loaded antenna offers improvements in gain and radiation efficiency, and it achieves an attractive peak gain of 7.87 dBi along with a maximum radiation efficiency of 98.8%. This suggested SPMA is a suitable choice for wireless communication applications at 2.4/5.2 GHz frequency bands.

The major contributions of this article are (i) Design of a staircase-shaped printed monopole antenna (SPMA) to support multiple wireless communication applications, (ii) Design of straight forward Jerusalem cross shaped 5×5 array to act as an FSS reflector, (iii) Radiation performance improvements in dual operating bands due to integration of frequency selective surface, and (iv) Dual operating bands to support modern wireless communication (WLAN/Wi-Fi etc.) applications at 2.4/5.2 GHz.

2. ANTENNA DESIGN METHODOLOGY

The transmission line model is used for designing the staircase-shaped printed monopole antenna. In order to operate at 2.4 GHz operating frequency, the patch sizes are calculated by applying mathematical equations, which are referred in [17–19].

The equations are implemented in MATLAB software to realize the required dimensions of the antenna. In this research work, a polyimide dielectric with a tangent loss of 0.0027, a 0.1 mm height, and a relative dielectric value of 3.5 was utilized for designing the proposed antenna. The patch's length (Lp) is 33.39 mm, and its width (Wp) is 41.66 mm which is obtained for given specifications of the dielectric substrate. After that, the antenna dimensions are optimized with the patch's length (Lp) 30 mm and its width (Wp) 16 mm, length of substrate (Ls) 49 mm and substrate width (Ws) = 29 mm in order to achieve a compact sized antenna. Later, the radiating patch of the antenna has been modified

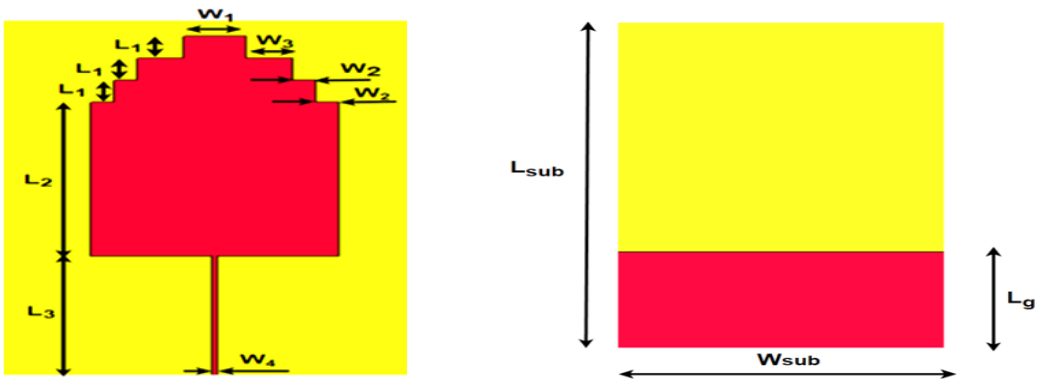

Figure 1. Proposed antenna (a) front side and (b) back side views.

by incorporating staircase-shaped slots along the vertical direction (length) on both sides of the required antenna. The patch's area has decreased by 7.5% because of these adjustments. After performing a parametric analysis for ground length, the proposed antenna operates at dual frequencies (2.4/5.2 GHz) with S_{11} magnitudes of -42.88 dB and -21.99 dB. The dimension of the antenna is $49 \times 29 \times 0.1\,\text{mm}^3$. The excitation to the staircase-shaped printed monopole antenna (SPMA) is provided via a 16.5 mm feed line, which is shown in Figure 1. The numerical performance analysis of the antenna can be done by using Computer Simulation Technology (CST) Microwave Studio, which uses finite-difference time-domain (FDTD) technique to give the solution accurately for Maxwell's equations. The geometrical layout of the proposed SPMA is shown in Figure 1 along with the dimensions of the design parameters listed in Table 1.

Table 1. Design parameters of the proposed antenna (All are in mm).

Parameter	Dimension
L_1	3.0
L_2	21.0
L_3	16.5
W_1	4.0
W_2	1.5
W_3	3.0
W_4	0.4
L_{Sub}	49.0
W_{Sub}	29.0
L_g	15.0

3. UNIT CELL DESIGN

The proposed unit cell contains an overall size of $16 \times 16\,\text{mm}^2$. A copper material, which is indicated with yellow color in Figure 2, is chosen as a conductive patch for designing the proposed unit cell structure. At first, a simple cross shape is taken as a radiating patch. Later by bending the cross-shaped arms, which is as shown in Figure 2, the initial cross shape will become like a Jerusalem cross. Figure 4 shows the reflection coefficient (S_{11}) plot for the proposed unit cell structure. To achieve compactness, a polyimide dielectric substrate has been used. One of the electromagnetic (EM) numerical simulation tools, CST Microwave Studio, is utilized to obtain numerical simulation response very quickly and

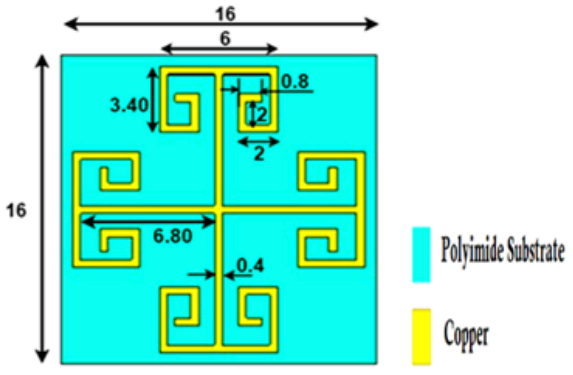

Figure 2. Unit cell of the proposed FSS (All dimensions are in mm).

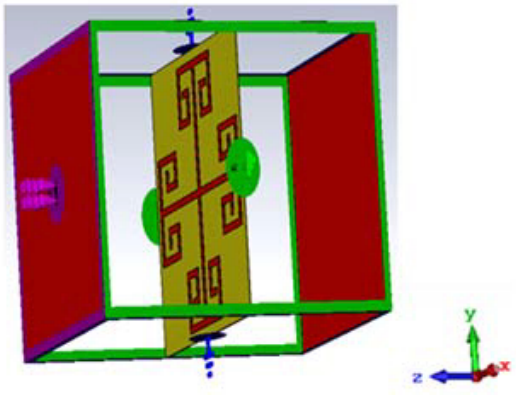

Figure 3. Snapshot of simulation set up for the proposed unit cell.

precisely [20]. The CST time domain solver has a key advantage in that the resource required grows linearly with the number of nodes. As a result, large structures like arrays with hundreds of radiating elements can be handled. To begin the simulation, the frequency range is selected in the simulation setup, and perfect electric and magnetic conditions are applied along the X and Y axes, respectively, to propagate the EM wave along the z-axis, as shown in Figure 3. As shown in Figure 4, the unit cell resonates from 1.2 GHz to 5.85 GHz providing an overall bandwidth of 4.65 GHz, while the measured S_{11} resonates from 1.38 GHz to 5.89 GHz.

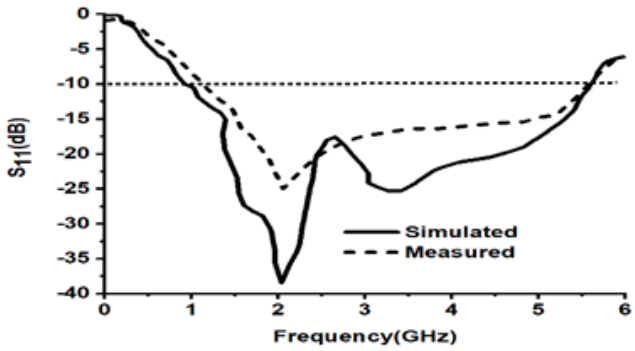

Figure 4. Reflection coefficients (S_{11}) of the suggested unit cell.

4. RESULTS AND DISCUSSION

The frequency-selective surface (FSS) is designed by repeating the structured unit cells in two directions (x and y). To optimize the FSS, many array combinations have been verified including 2×2, 4×4, 5×5, 7×7, 8×8, and 10×10 sizes, and different air space dimensions between the antenna and FSS reflector are investigated such as 5, 8, 10, 15, and 20 mm. Out of all these, 10 mm for the 5×5 array size is the best configuration that offers better gain and efficiency for the antenna and reflector combination. The total dimension of the proposed FSS is 80 mm $\times$ 80 mm. The fabricated prototypes of the antenna with front and back views are shown in Figures 5(a)–(b), and the prototype of the FSS is depicted in the Figure 5(c).

Parametric analysis for various distances between the antenna and FSS is investigated, and the variations in S_{11} are shown in Figure 6. The S_{11} (dB) is evaluated in CST studio utilizing parametric sweep analysis with different air space cases present between the antenna and reflector to get maximum performance. As shown in Figure 6, with a 5 mm air space between the reflector and antenna, its combination resonates at 2.4 and 4.32 GHz, with S_{11} values of -21.2 and -22.5 dB, respectively. When the spacing is expanded to 8 mm, it resonates at 1.52 and 4.32 GHz with S_{11} values of -20.5 and -22.46 dB, respectively. For a 10 mm air space between the antenna and FSS, the obtained frequencies are 2.52 and 5.2 GHz with S_{11} parameter values of -35.5 and -24.6 dB, respectively, which is indicated by a black-colored solid line. Resonances are observed at 1.32 GHz and 4.12 GHz for a 15 mm air space, with S_{11} values of -22.4 dB and -21.8 dB, respectively. Finally, the structure resonates at 1.32 GHz and 4.12 GHz for a 20 mm air space, with S_{11} values of -15.2 dB and -15.6 dB, respectively. In all the above cases, the space of 10 mm has given better gain and radiation efficiency. Here, a black-colored solid line indicates the required 10 mm separation gap between the antenna and FSS to obtain the optimum performance. The measuring setup for the combinations of antenna and FSS model is shown in Figure 7. When the patch structure is simulated alone, the obtained S_{11} values are -42.88 dB at 2.4 GHz and -21.99 dB at 5.2 GHz frequency, respectively. However, with measurement the antenna resonates at 2.52 and 5.2 GHz frequencies with S_{11} values -35.5 and -24.6 dB, respectively. As shown in Figure 8, resonances are observed for antenna and FSS combination at dual frequencies (2.3, 5 GHz) with S_{11} magnitudes of -28.2 dB and -20 dB, respectively, whereas measured resonances are observed for antenna and FSS combination at dual frequencies (2.3, 5 GHz), with S_{11} magnitudes of -25.8 and -22.20 dB, respectively. Here, the red-colored solid line indicates the simulated S-parameter for the

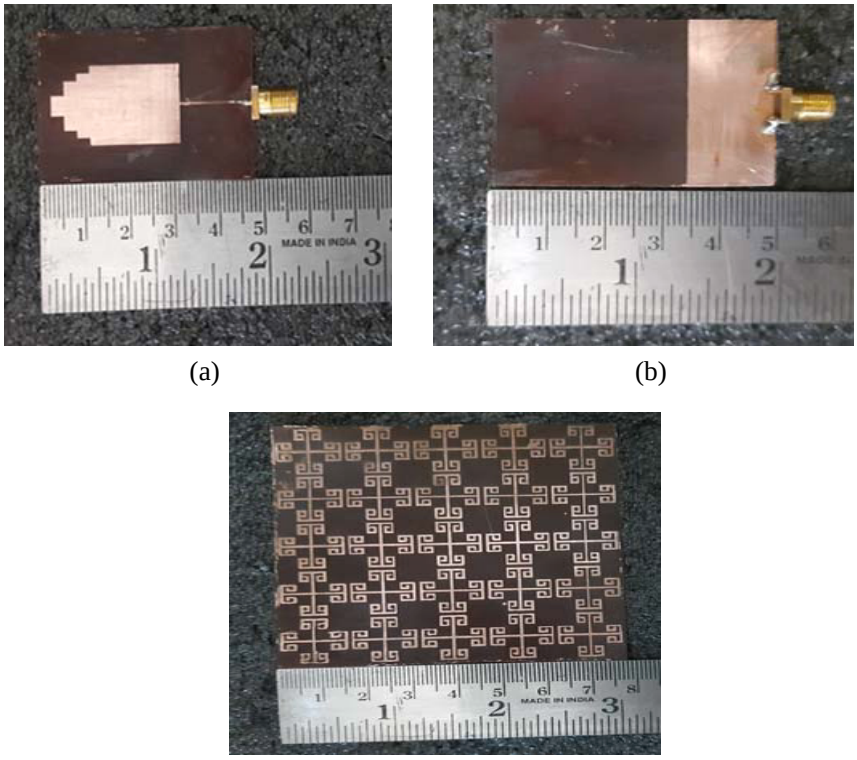

Figure 5. Fabricated prototypes. (a) Antenna front side. (b) Antenna back side. (c) Proposed FSS with 5×5 array size.

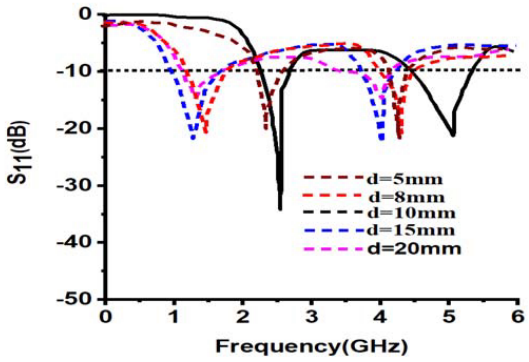

Figure 6. Parametric analysis for various distances (d) between antenna and FSS.

antenna alone; the red-colored dotted line indicates the measured reflection coefficient for the antenna alone; the black colored solid line indicates the measured return loss plot; and the black colored dotted line indicates the simulated S-parameter for the antenna integrated with FSS structure.

From Figure 9, it can be noted that the red-colored solid line indicates simulated gain with FSS, and the red-colored short-dashed line indicates measured gain with FSS. Similarly, the black-colored solid line indicates simulated gain for the antenna without FSS, and the black-colored short-dashed line indicates measured gain for the antenna without FSS. From Figure 9 and Figure 10, it can be noted that the radiation efficiency is nearly 98% at 5 GHz and 98.8% at 2.4 GHz for the antenna and reflector integration. At 5.2 GHz, the maximum gain is noted as 7.87 dBi while at 2.4 GHz, it is 3.38 dBi for the proposed antenna and reflector integration. An improvement can be observed in gain and efficiency at

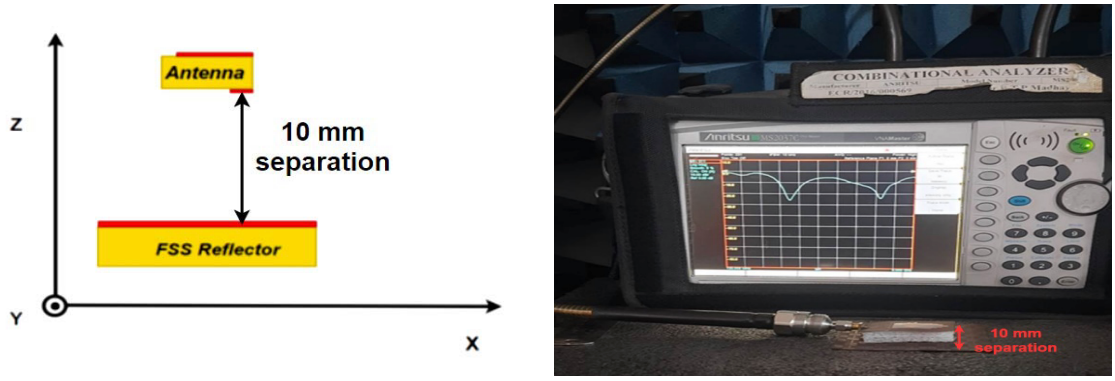

(a) (b)

Figure 7. The measurement set up, (a) gap of 10 mm between the antenna and FSS reflector, (b) separation with a sponze as a space layer between FSS and antenna.

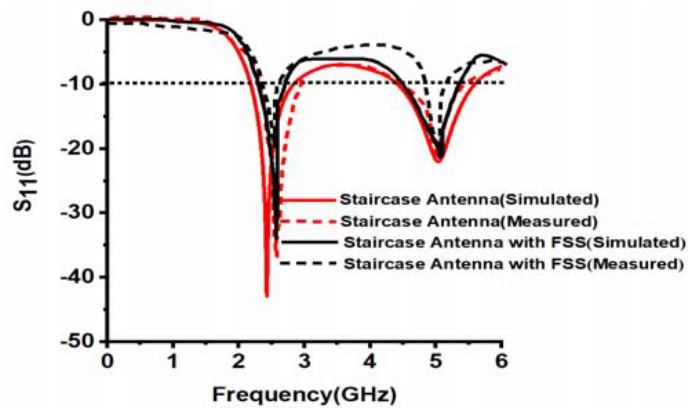

Figure 8. Reflection coefficient (S_{11}) plots for simulation and measurement using both FSS and without FSS.

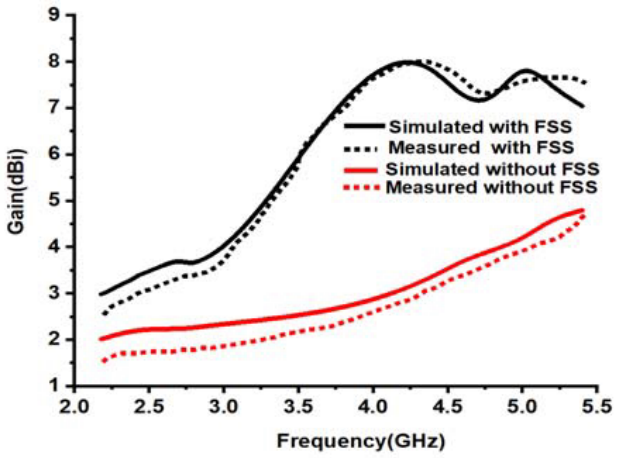

Figure 9. Gain variations for without FSS and with FSS.

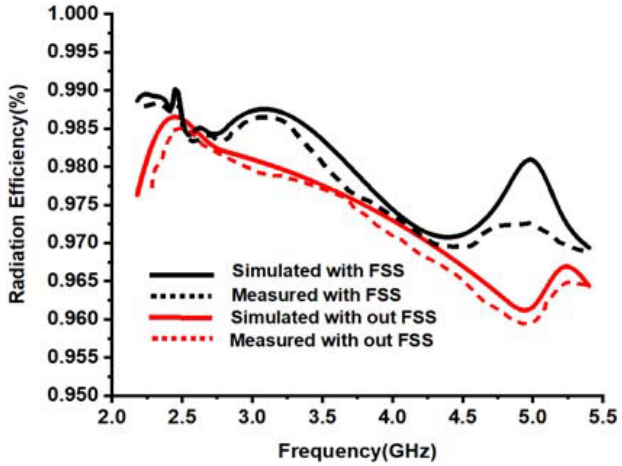

Figure 10. Radiation efficiency with and without FSS.

Table 2. Comparison table for simulated radiation parameters.

	Using Antenna		Using Antenna with FSS	
Parameter	2.4 GHz	5.2 GHz	2.4 GHz	5.2 GHz
Gain	2.22	4.19	3.38	7.87
Efficiency (%)	98.6	96.1	98.8	98

Table 3. Comparison table for measured gain and efficiency parameters.

	Using Antenna		Using Antenna with FSS	
Parameter	2.4 GHz	5.2 GHz	2.4 GHz	5.2 GHz
Gain	1.72	4.13	3.32	7.58
Efficiency (%)	98.3	96.07	98.7	97.4

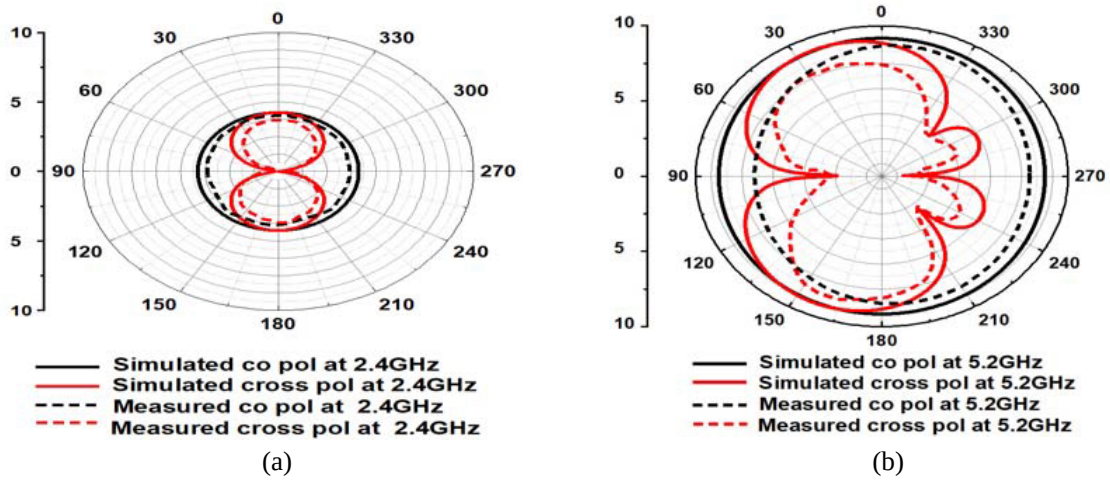

Figure 11. *E*-plane field patterns for (a) 2.4 and (b) 5.2 GHz frequencies without FSS reflector.

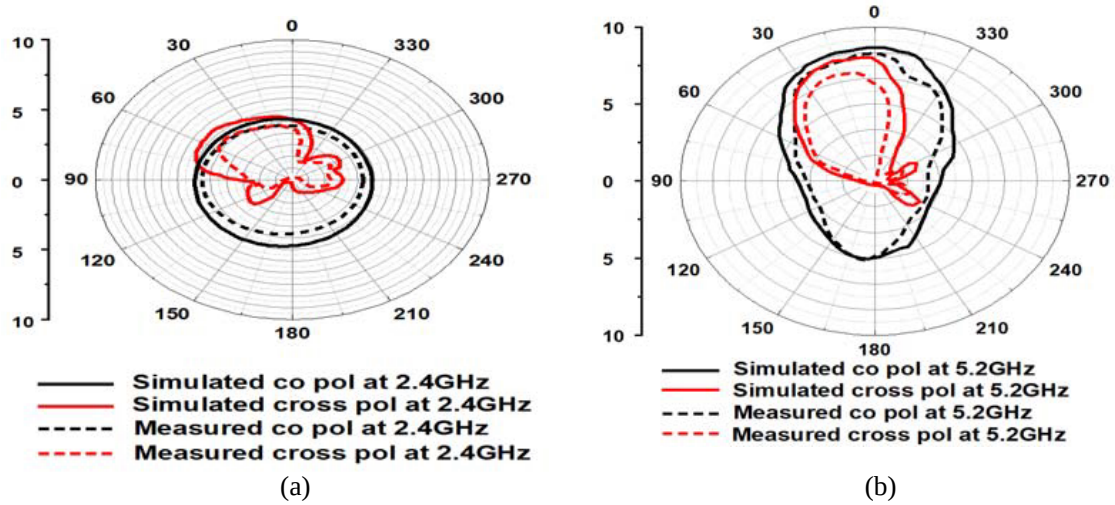

Figure 12. *E*-plane field patterns at (a) 2.4 and (b) 5.2 GHz frequencies using FSS reflector.

wireless resonant frequencies for an integrated antenna. The comparisons of all radiation parameters for the stair-case antenna with or without FSS in terms of simulated and measured results are represented in Table 2 and Table 3. Figures 11 and 12 illustrate the radiation patterns for the proposed SPMA and the combination of SPMA with the proposed FSS reflector at both resonant frequencies. From figure 12, it can be noted that, by positioning the proposed FSS reflector beneath the antenna with an air gap of 10 mm, the FSS reflects the EM waves imposed on it, resulting in the SPMA's unidirectional radiation pattern.

4.1. Equivalent Circuit Model of the Proposed Antenna

Antennas, in general, exhibit a linear behavior since they are made up of passive elements that resonate at various frequencies. The first Foster canonical form [21] is ideal for modeling antennas such as dipoles and monopoles. The entire staircase-shaped printed monopole antenna (SPMA) is depicted with an equivalent approach using the advanced design system (ADS) tool. It can be noted From Figure 13 that $L1$ represents the whole radiating patch of the antenna structure, and the partial ground of the antenna is represented as a short circuit. As indicated in Figure 13, a parallel R-L-C combination is used for producing numerous resonant frequencies in the ADS tool. To produce the exact S-parameter response shown in Figure 14, a 50-ohm impedance is attached to the radio frequency (RF) feed to ensure adequate impedance matching for the coaxial feed. With coaxial feed, the dielectric constant and loss tangent are fixed. To achieve optimal performance, the parallel RLC (PRLC) and remaining parameters in the coaxial feed are optimized by utilizing the ADS tool's tuning feature. To get the appropriate return loss (S_{11}) response, the start and end frequencies are set to 0 GHz and 6 GHz, respectively, with a 0.1 GHz frequency step size. From Figure 14, it can be noted that the frequency range is specified on the X-axis from 0 to 6 GHz, and the S_{11} (dB) is chosen on the Y-axis. The red curve represents the simulated response using the CST tool, and the black curve represents the return loss response of a similar circuit in the ADS tool. According to the projected graph, the CST and the ADS tool responses for S_{11} parameters are almost identical.

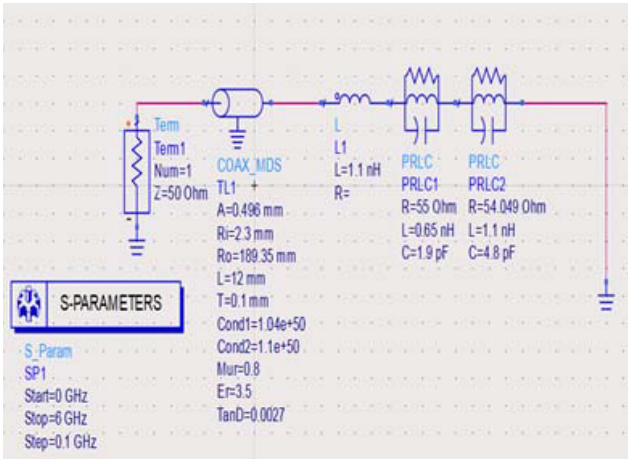

Figure 13. Equivalent LC circuit model for the antenna.

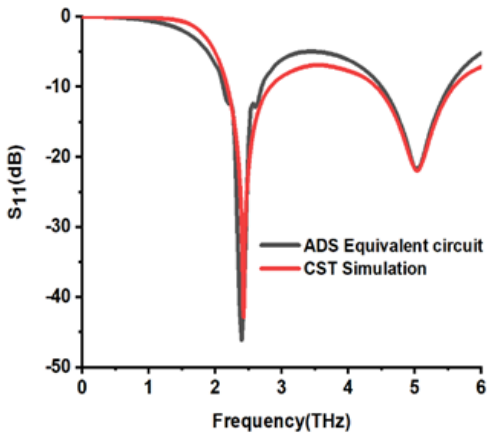

Figure 14. S_{11} comparison using CST and ADS tools.

4.2. *E*-, *H*-Fields and Surface Current Distribution Analysis

Figure 15 shows that at 2.4 GHz, the maximum intensity of the electric field is noticed on the staircases of the radiating patch and spreads along the vertical direction of the antenna. Figure 16 shows that a maximal magnetic field is seen on the feed line and that it spreads in the horizontal direction of the antenna at a 2.4 GHz frequency. As a result, the electric and magnetic fields spread in opposite

directions. Similarly, at 5.2 GHz, the highest electric field is detected on the feed line and in the horizontal direction, whereas the magnetic field spreads in the vertical direction. According to Figure 17, a maximum current distribution is detected on the feed line for 2.4 GHz operation, and at 5.2 GHz frequency, the surface current distribution spreads along the horizontal direction, with the lowest current distribution observed on the corners of the staircase-shaped radiating patch.

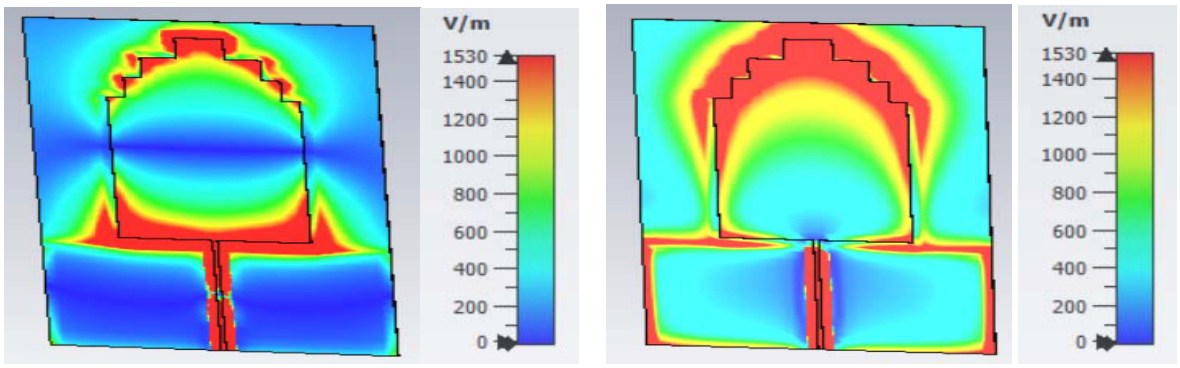

(a) (b)

Figure 15. *E*-field distribution at dual frequencies (a) 2.4, (b) 5.2 GHz.

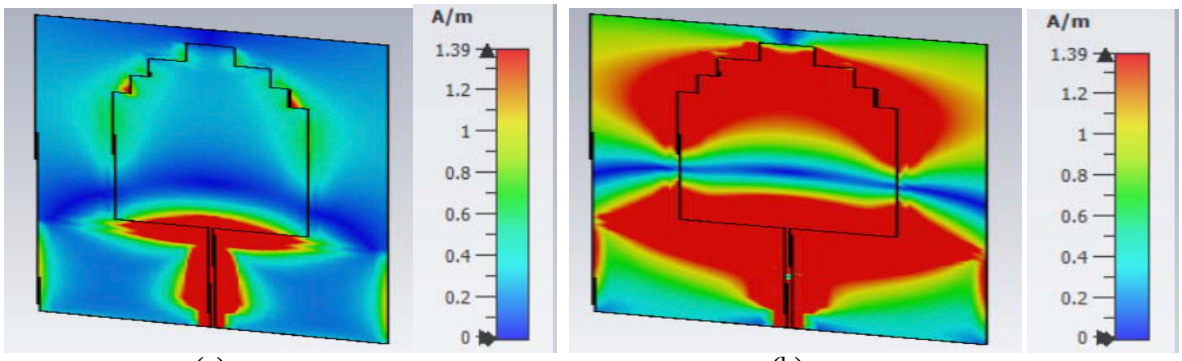

(a) (b)

Figure 16. *H*-field distribution at dual frequencies (a) 2.4, (b) 5.2 GHz.

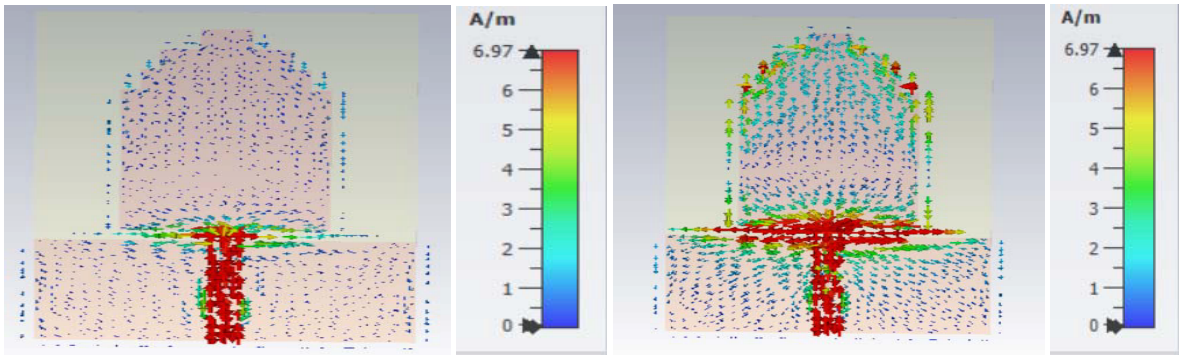

(a) (b)

Figure 17. Surface current distributions at dual frequencies (a) 2.4, (b) 5.2 GHz.

4.3. Performance Comparison with Other Reported Works

The FSS integrated antenna performance has been evaluated in comparison to the presented literature, which is represented in Table 4. This proposed staircase-shaped printed monopole antenna (SPMA) offers acceptable performance in terms of gain, impedance bandwidth, gain, and radiation efficiency by maintaining compact size.

Table 4. Comparison with recently reported work.

Ref.	Antenna Dimension (mm^3)	Frequency Bands (GHz)	Fractional Bandwidth (%)	Peak Gain (dBi)
[13]	$40 \times 40 \times 1.6$	(2.37–2.56) and (5.15–6.22)	7% and 18.8%	7.46
[14]	$44 \times 35 \times 1.6$	(3.48–3.65) and (5.75–6.37)	4.8% and 10%	13.92
[15]	$45 \times 42 \times 2.7$	$f_r = 3.09$ and 6	—	7.5 and 10.95
[16]	$42.5 \times 28.5 \times 1.575$	(2.41–2.62) and (3.38–3.65)	8.3% and 7.6%	10.2 and 8.83
This Work	$49 \times 29 \times 0.1$	(2.18–2.83) and (4.42–5.58)	25.94% and 23.2%	7.87

5. CONCLUSIONS

This article introduces a staircase-shaped printed monopole antenna (SPMA) for the usage in wireless frequency bands. The combination of single-layer FSS and proposed SMPA achieves high radiation parameters in comparison to the single SMPA alone. The overall dimensions of the antenna and FSS are $49 \times 29 \times 0.1\,mm^3$ and $80 \times 80 \times 0.135\,mm^3$, respectively. The polyimide dielectric substrate material has been implemented for simulation design and the execution of the prototype modeling of both the antenna and FSS reflector. The designed FSS with optimized dimensions produces a better outcome which results in satisfactory antenna performance. For 2.4 and 5.2 GHz frequencies, the suggested antenna and reflector combination achieve 25.94% and 23.2% fractional bandwidths, respectively. This study's results seem satisfactory compared to other reported research works as provided in the comparison table. Hence, this SPMA is a suitable choice for wireless communications at 2.4/5.2 GHz frequency bands to support WLAN and Wi-Fi applications.

ACKNOWLEDGMENT

Authors like to acknowledge the DST through technical support from SR/PURSE/2023/196 & SR/FST/ET-II/2019/450.

REFERENCES

1. Kumar, J., B. Basu, F. A. Talukdar, and A. Nandi, "Stable-multiband frequency reconfigurable antenna with improved radiation efficiency and increased number of multiband operations," *IET Microwaves, Antennas & Propagation*, Vol. 13, No. 5, 642–648, Apr. 2019.
2. Nehra, R. K. and N. S. Raghava, "Compact dual-band Zig Zag shaped implantable antenna for biomedical devices," *Indian Journal of Pure & Applied Physics (IJPAP)*, Vol. 60, No. 10, 841–848, 2022.

3. Ayoub, A. F., "Analysis of rectangular microstrip antennas with air substrates," *Journal of Electromagnetic Waves and Applications*, Vol. 17, No. 12, 1755–1766, 2003.
4. Wang, W. and Y. Zheng, "Improved design of the Vivaldi dielectric notch radiator with etched slots and a parasitic patch," *IEEE Antennas and Wireless Propagation Letters*, Vol. 17, No. 6, 1064–1068, Jun. 2018, doi: 10.1109/LAWP.2018.2832098.
5. Wang, C., L. Wang, Y. Zhang, W. Hu, and X. Jiang, "A filtering dielectric resonator antenna using CPW fed for sub-6 GHz applications," *Progress In Electromagnetics Research Letters*, Vol. 105, 49–56, 2022.
6. Latif, S. I., L. Shafai, and C. Shafai, "Gain and efficiency enhancement of compact and miniaturised microstrip antennas using multi-layered laminated conductors," *IET Microwaves, Antennas & Propagation*, Vol. 5, No. 4, 402–411, 2011.
7. Sheng, X., X. Lu, N. Liu, and Y. Liu, "Design of broadband high-gain Fabry-Pérot antenna using frequency-selective surface," *Sensors*, Vol. 22, 9698, 2022.
8. Mondal, K., "A novel-shaped reduced size FSS-based broadband high gain microstrip patch antenna for WiMAX/WLAN/ISM/X-band applications," *Journal of Circuits, Systems and Computers*, Vol. 30, No. 16, 2150290, Dec. 30, 2021.
9. Zhang, J.-J., B. Wu, Y.-T. Zhao, L. Song, H.-R. Zu, R.-G. Song, and D.-P. He, "Two-dimensional highly sensitive wireless displacement sensor with bilayer graphene-based frequency selective surface," *IEEE Sensors Journal*, Vol. 21, No. 21, 23889–23897, 2021.
10. Ashyap, A. Y. I., Z. Z. Abidin, S. H. Dahlan, H. A. Majid, M. R. Kamarudin, A. Alomainy, R. A. Abd-Alhameed, J. S. Kosha, and J. M. Noras, "Highly efficient wearable CPW antenna enabled by EBG-FSS structure for medical body area network applications," *IEEE Access*, Vol. 6, 77529–77541, 2018.
11. Das, P. and K. Mandal, "Passive FSS based polarization converter integrated microstrip antenna," *International Journal of RF and Microwave Computer-Aided Engineering*, Vol. 32, No. 2, e22982, Feb. 2022.
12. Boukern, D., A. Bouacha, D. Aissaoui, M. Belazzoug, and T. A. Denidni, "High-gain cavity antenna combining AMC-reflector and FSS superstrate technique," *International Journal of RF and Microwave Computer-Aided Engineering*, Vol. 31, No. 7, e22674, 2021.
13. Fernandes, E. M. F., M. W. B. da Silva, L. da Silva Briggs, A. L. P. de Siqueira Campos, H. X. de Araújo, I. R. S. Casella, C. E. Capovilla, V. P. R. M. Souza, and L. J. de Matos, "2.4–5.8 GHz dual-band patch antenna with FSS reflector for radiation parameters enhancement," *AEU-International Journal of Electronics and Communications*, Vol. 108, 235–241, 2019.
14. Sah, S., A. Mittal, and M. R. Tripathy, "High gain dual band slot antenna loaded with frequency selective surface for WLAN/fixed wireless communication," *Microwave and Optical Technology Letters*, Vol. 61, No. 2, 519–525, 2019.
15. Ballav, S., A. Chatterjee, and S. K. Parui, "Gain augmentation of a dual-band dielectric resonator antenna with frequency selective surface superstrate," *International Journal of RF and Microwave Computer-Aided Engineering*, Vol. 31, No. 4, e22575, 2021.
16. Ashvanth, B., B. Partibane, M. G. Alsath, and R. Kalidoss, "Gain enhanced multipattern reconfigurable antenna for vehicular communications," *International Journal of RF and Microwave Computer-Aided Engineering*, Vol. 30, No. 6, e22192, Jun. 2020.
17. Marhoon, H. M., N. Qasem, N. Basil, and A. R. Ibrahim, "Design and simulation of a compact metal-graphene frequency reconfigurable microstrip patch antenna with FSS superstrate for 5G applications," *International Journal on Engineering Applications*, Vol. 10, 193–201, 2022.
18. Ali, T., M. M. Khaleeq, and R. C. Biradar, "A multiband reconfigurable slot antenna for wireless applications," *AEU-International Journal of Electronics and Communications*, Vol. 84, 273–280, Feb. 1, 2018.
19. Devarapalli, A. B. and T. Moyra, "Design of a metamaterial loaded W-shaped patch antenna with FSS for improved bandwidth and gain," *Silicon*, 1–4, Oct. 10, 2022.

20. Paula, A. L., M. C. Rezende, and J. J. Barroso, "Experimental measurements and numerical simulation of permittivity and permeability of teflon in X band," *Journal of Aerospace Technology and Management*, Vol. 3, 59–64, Jan. 2011.
21. Meher, P. R. and S. K. Mishra, "Design and development of mathematical equivalent circuit model of broadband circularly polarized semi-annular ring-shaped monopole antenna," *Progress In Electromagnetics Research C*, Vol. 129, 73–87, 2023.